

Learning Latent Energy-Based Models via Interacting Particle Langevin Dynamics

Joanna Marks*, Tim Y. J. Wang* and O. Deniz Akyildiz

Department of Mathematics, Imperial College London

{joanna.marks23, yunjie.wang20, deniz.akyildiz}@imperial.ac.uk

October 15, 2025

Abstract

We develop interacting particle algorithms for learning latent variable models with energy-based priors. To do so, we leverage recent developments in particle-based methods for solving maximum marginal likelihood estimation (MMLE) problems. Specifically, we provide a continuous-time framework for learning latent energy-based models, by defining stochastic differential equations (SDEs) that provably solve the MMLE problem. We obtain a practical algorithm as a discretisation of these SDEs and provide theoretical guarantees for the convergence of the proposed algorithm. Finally, we demonstrate the empirical effectiveness of our method on synthetic and image datasets.

1 Introduction

Energy-Based Models (EBMs) offer a flexible framework for statistical and generative modelling by learning models of the form $p_\theta \propto e^{-U_\theta}$ from data. The energy function U_θ can be flexibly parameterised, enabling EBMs to approximate any probability density (Atchadé et al., 2023). Once the parameters θ are learned for a given dataset, these models support sampling and inference, allowing their use in a wide range of applications, including generation across modalities (Deng et al., 2021; Gladstone et al., 2025), robust classification (Grathwohl et al., 2020), anomaly detection (Zhai et al., 2016), likelihood-based evaluation (Du and Mordatch, 2019), simulation-based inference (Glaser et al., 2022), and compositional generation (Du et al., 2020, 2023).

Maximum Likelihood Estimation (MLE) procedures to learn EBMs remain highly challenging to implement since common methods require samples from the model p_θ to perform parameter updates, typically drawn using Markov chain Monte Carlo (MCMC) methods (Hinton, 2002; Song and Kingma, 2021). In high dimensional settings, these often suffer from slow mixing times. Moreover, real-world data often concentrates on a low-dimensional manifold embedded in a high-dimensional data space (Bengio et al., 2013; Whiteley et al., 2025), meaning that the learning task might be ill-defined (Loaiza-Ganem et al., 2024).

To exploit the low-dimensional data structure Latent Variable Models (LVMs) have been studied. In the EBM framework, one approach is to model the system as a LVM, where a flexible energy-based prior is defined over the latent space and a neural network decoder maps latent variables to the data space; this setup is known as a Latent Energy-Based Model (LEBM) (Pang et al., 2020).

*These authors contributed equally.

Significant challenges remain, however, in the training of such models via MLE. First, the model parameters must be learned by maximising the *marginal likelihood* of the observed data, which involves integrating out the latent variables, a typical setting known as Maximum Marginal Likelihood Estimation (MMLE) (Dempster et al., 1977). Second, the normalising constant of the prior distribution is generally intractable, resulting in a “doubly-intractable” setting.

A notable work in the direction of MLE for LEBMs is Pang et al. (2020), who propose an MCMC-based approach to tackle both the intractable posterior and the intractable normalising constant of the prior. This procedure can be seen as an Expectation-Maximization (EM)-like procedure, in a similar spirit to De Bortoli et al. (2021). Adapted to the EBM setting, these methods involve inner MCMC loops to sample from the posterior and/or the prior at each iteration of the training. However, the nested MCMC steps lead to slow training and complicate theoretical understanding of the model; which is the main motivation for our work.

In this work, we introduce a novel, diffusion-based approach for MMLE problem for the EBM prior latent variable model. By leveraging the rich connection between Langevin dynamics and optimisation (Raginsky et al., 2017; Zhang et al., 2023), we develop a training algorithm based on an interacting particle system that simultaneously estimates the parameters and the posterior distribution through solving a system of SDEs.

Contributions. Our contributions can be summarised as follows:

- We introduce a continuous-time, SDE-based framework for training latent EBMs. This interacting particle system is inspired by the Interacting Particle Langevin Algorithm (IPLA) (Akyildiz et al., 2025) and adapted to the LEBM setting. Specifically, in Section 3, we develop an algorithm by discretising SDE systems that target the MMLE solution, termed Energy-Based Interacting Particle Langevin Algorithm (EBIPLA), given in Algorithm 1.
- We then provide non-asymptotic analysis for our method in Section 4 under log-concavity and smoothness assumptions. We show that the parameter estimates $(\theta_k)_{k \geq 0}$ generated by EBIPLA converge to the optimal parameter θ_* as the number of data points and the particles in our method grow, under a variety of settings. These results constitute the first convergence bounds for training LEBMs.
- In Section 6, we empirically validate the effectiveness of our method on synthetic datasets and image generation tasks, showing that it achieves competitive performance among relevant baselines.

Notation. We use $\mathcal{O}(\cdot)$ to denote upper bounds up to constant factors, and $\tilde{\mathcal{O}}(\cdot)$ to denote the same while suppressing polylogarithmic terms. For a random variable X , the notation $\mathcal{L}(X)$ denotes the law (distribution) of X while $\sigma(X)$ denotes the σ -algebra generated by X . For any two probability distributions μ and ν , we define the Wasserstein distance:

$$W_2(\mu, \nu) := \left(\inf_{\gamma \in \Gamma(\mu, \nu)} \int \|x - y\|^2 d\gamma(x, y) \right)^{1/2},$$

where $\Gamma(\mu, \nu)$ is the set of all couplings of μ and ν . The notation δ_x denotes the Dirac measure at x . Where appropriate, we use the notation $x^{1:M} = \{x^m\}_{m=1}^M$ and $x^{1:M, 1:N} = \{x^{m,n}\}_{m=1, n=1}^{M, N}$ to denote collections of variables.

2 Background

We start by defining a real-valued latent energy-based probabilistic model (Pang et al., 2020; Yu et al., 2023):

$$p_\theta(x, y) = p_\alpha(x)p_\beta(y | x), \quad (1)$$

where $\theta = (\alpha, \beta) \in \mathbb{R}^{d_\alpha + d_\beta} = \mathbb{R}^{d_\theta}$ and $p_\beta(y|x) = \mathcal{N}(y; g_\beta(x), \sigma^2 I)$ is an isotropic Gaussian distribution. Here, $g_\beta : \mathbb{R}^{d_x} \rightarrow \mathbb{R}^{d_y}$ denotes a generator function parametrised by β that maps from the latent space to the ambient space. The prior $p_\alpha(x)$ is modeled as an EBM:

$$p_\alpha(x) = \frac{1}{Z(\alpha)} e^{-U_\alpha(x)}, \quad (2)$$

where $Z(\alpha) = \int e^{-U_\alpha(x)} dx$ is the α -dependent normalising constant. When $U_\alpha(x)$ is chosen to be a neural network, the EBM can capture meaningful latent structures.

2.1 Maximum marginal likelihood estimation

Given a dataset $\{y_m\}_{m=1}^M \sim p_{\text{data}}$, we are interested in learning the parameters θ of the model by maximising the marginal likelihood of the observed data. This problem is termed the MMLE problem. Specifically, we want to solve

$$\theta_*^{\text{pop}} \in \arg \max_{\theta \in \mathbb{R}^{d_\theta}} \ell(\theta), \quad \ell(\theta) := \mathbb{E}_{p_{\text{data}}} [\log p_\theta(Y)].$$

where

$$p_\theta(y) = \int p_\alpha(x) p_\beta(y|x) dx.$$

Since we do not have access to the data distribution p_{data} , we can approximate the expectation over p_{data} by an empirical measure $p_{\text{data}}^M = (1/M) \sum_{m=1}^M \delta_{y_m}(dy)$ which yields the empirical loss function

$$\ell_M(\theta) = \frac{1}{M} \sum_{m=1}^M \log p_\theta(y_m) \quad (3)$$

converting the population MMLE problem to the empirical MMLE problem:

$$\theta_* \in \arg \max_{\theta \in \mathbb{R}^{d_\theta}} \frac{1}{M} \sum_{m=1}^M \log p_\theta(y_m), \quad (4)$$

where M denotes the number of data-points. Our main goal in this paper is to solve (4) efficiently and to provide theoretical guarantees for the obtained solution.

2.2 Optimisation via Langevin dynamics

Following [Akyildiz et al. \(2025\)](#), in order to maximise $\ell(\theta)$, we will exploit stochastic dynamics whose long-run behavior naturally concentrates around the maximisers. A classical choice is *Langevin dynamics*, given by the SDE ([Raginsky et al., 2017](#); [Zhang et al., 2023](#))

$$d\theta_t = \nabla_\theta \ell(\theta_t) dt + \sqrt{2/\eta} dB_t, \quad (5)$$

where $(B_t)_{t \geq 0}$ is a standard d_θ -dimensional Brownian motion and $\eta > 0$ is an inverse temperature parameter. This SDE admits an invariant measure $\pi(\theta) \propto \exp(\eta \ell(\theta))$ so that for large η , $\pi(\theta)$ concentrates around the maximisers of $\ell(\theta)$ ([Hwang, 1980](#)).

3 The Algorithm

In practice, simulating Langevin dynamics given in (5) requires repeated evaluations of $\nabla_\theta \ell(\theta)$; we therefore turn to how this gradient can be estimated in the marginal likelihood setting. We note that, by using Fisher's identity ([Douc et al., 2014](#), Proposition D.4) for $\nabla_\theta \log p_\theta(y)$, we have

$$\nabla_\theta \ell(\theta) = \mathbb{E}_{p_{\text{data}}} \mathbb{E}_{p(\cdot|Y)} [\nabla \log p_\theta(\cdot, Y)]. \quad (6)$$

Replacing p_{data} with the empirical distribution p_{data}^M , we can estimate the gradient in (6) with

$$\nabla_{\theta} \ell_M(\theta) = \frac{1}{M} \sum_{m=1}^M \mathbb{E}_{p_{\theta}(\cdot|y_m)} [\nabla \log p_{\theta}(\cdot, y_m)].$$

This gradient remains intractable as $p(\cdot|y_m)$ is a posterior distribution which is typically not available in closed form. A typical workaround is to use MCMC to sample from $p_{\theta}(\cdot|y_m)$ (Pang et al., 2020; De Bortoli et al., 2021). We will instead follow Akyildiz et al. (2025), Kuntz et al. (2023) and use a particle approach where a set of N particles will target the posterior $p_{\theta}(\cdot|y_m)$ for each data point y_m . We denote these particles as $X_t^{m,n}$, where $m \in \{1, \dots, M\}$ indexes the data point and $n \in \{1, \dots, N\}$ indexes the particle.

3.1 An Interacting Particle Algorithm

Define a function $\phi_y : \mathbb{R}^{d_y} \times \mathbb{R}^{d_x} \times \mathbb{R}^{d_{\theta}} \rightarrow \mathbb{R}$ as $\phi_y(\theta, x) = -\log p_{\theta}(x, y)$. We choose the noise scaling in (5) to be $\eta = MN$, which ensures that the SDE admits an invariant measure which concentrates around the maximisers of $\ell_M(\theta)$ with both increasing number of particles N as well as increasing number of data points M . Specifically, for each data point y_m , we evolve N particles, denoted $X_t^{m,n}$ for $n = 1, \dots, N$, according to Langevin dynamics targeting the posterior $p_{\theta}(\cdot|y_m)$. Simultaneously we use the particles estimate the gradient $\nabla_{\theta} \ell_M(\theta)$ and evolve θ according to Langevin dynamics targeting the maximisers of $\ell_M(\theta)$.

Let us denote the joint empirical measure of the particles and data points as $\mathbf{p}_t^{MN} = (1/MN) \sum_{m=1}^M \sum_{n=1}^N \delta_{(y_m, X_t^{m,n})}$. Using this, we propose to use the following SDE system:

$$d\theta_t = -\mathbb{E}_{\mathbf{p}_t^{MN}} [\nabla_{\theta} \phi_Y(\theta_t, X)] dt + \sqrt{\frac{2}{MN}} dB_t, \quad (7)$$

$$dX_t^{m,n} = -\nabla_x \phi_{y_m}(\theta_t, X_t^{m,n}) dt + \sqrt{2} dB_t^{m,n}, \quad (8)$$

where $(B_t)_{t \geq 0}$ is a d_{θ} -dimensional Brownian motion and $(B_t^{m,n})_{t \geq 0}$ for $m \in \{1, \dots, M\}$, $n \in \{1, \dots, N\}$ denote a family of d_x -dimensional independent standard Brownian motions. This is a generalisation of the interacting particle system introduced in Akyildiz et al. (2025) to M data point setting. One can observe that Eq. (7) aligns with the global optimisation setting given in Eq. (5) with the choice of $\eta = MN$.

In order to construct an implementable algorithm, we discretise the SDEs (7)–(8) using an Euler–Maruyama discretisation. Given a (possibly random) initial value θ_0 and particles $X_0^{1:M, 1:N}$, a step size $h > 0$, the discretised system for $k \geq 1$ is given by

$$\theta_{k+1} = \theta_k - h \mathbb{E}_{\mathbf{p}_k^{MN}} [\nabla_{\theta} \phi_Y(\theta_k, X)] + \sqrt{\frac{2h}{MN}} W_k, \quad (9)$$

$$X_{k+1}^{m,n} = X_k^{m,n} - h \nabla_x \phi_m(\theta_k, X_k^{m,n}) + \sqrt{2h} W_k^{m,n}, \quad (10)$$

where $\mathbf{p}_k^{MN} = (1/MN) \sum_{m=1}^M \sum_{n=1}^N \delta_{(y_m, X_k^{m,n})}$ and $(W_k)_{k \geq 0}$ and $(W_k^{m,n})_{k \geq 0}$ for all $m \in \{1, \dots, M\}$, $n \in \{1, \dots, N\}$ denote independent standard Gaussian random variables of appropriate dimension¹. Specifically, the drift coefficient in (9) can be explicitly written as

$$\mathbb{E}_{\mathbf{p}_k^{MN}} [\nabla_{\theta} \phi_Y(\theta_k, X)] = \frac{1}{MN} \sum_{m=1}^M \sum_{n=1}^N \nabla_{\theta} \phi_{y_m}(\theta_k, X_k^{m,n}).$$

To connect this to the estimation task for our model given in (1), let us define the function $V_{\beta}(x, y) = -\log p_{\beta}(y|x)$. Given the energy function $U_{\alpha} : \mathbb{R}^{d_x} \rightarrow \mathbb{R}$, the gradient with respect to $\theta = (\alpha, \beta)$ should

¹With a slight abuse of notation, we use the same notation for the continuous time processes $(\theta_t, X_t^{m,n})$ and their discretisation $(\theta_k, X_k^{m,n})$.

be made explicit to clarify the implementation (for the derivation, see Appendix A). Written fully explicitly, we can rewrite the system in Eqs. (9)–(10) as

$$\alpha_{k+1} = \alpha_k - \frac{h}{MN} \sum_{n=1}^N \sum_{m=1}^M \nabla_\alpha U_{\alpha_k}(X_k^{m,n}) + h \mathbb{E}_{p_{\alpha_k}(x)}[\nabla_\alpha U_{\alpha_k}(x)] + \sqrt{\frac{2h}{MN}} W_k^\alpha, \quad (11)$$

$$\beta_{k+1} = \beta_k - \frac{h}{MN} \sum_{n=1}^N \sum_{m=1}^M \nabla_\beta V_{\beta_k}(X_k^{m,n}, y_m) + \sqrt{\frac{2h}{MN}} W_k^\beta, \quad (12)$$

$$X_{k+1}^{m,n} = X_k^{m,n} - h \nabla_x U_{\alpha_k}(X_k^{m,n}) - h \nabla_x V_{\beta_k}(X_k^{m,n}, y_m) + \sqrt{2h} W_k^{m,n} \quad (13)$$

for all $k \in \{1, \dots, K\}$, where $(W_k^\alpha)_{k \geq 0}$, $(W_k^\beta)_{k \geq 0}$, and $(W_k^{m,n})_{k \geq 0}$ denote independent standard Gaussian random variables of appropriate dimension. Note that the update for α in (11) involves an expectation with respect to the prior, i.e. $\mathbb{E}_{p_{\alpha_k}(x)}[\nabla_\alpha U_{\alpha_k}(x)]$, which originates from the normalising constant Z_α (see Appendix A for details). As this expectation is generally intractable, it must also be approximated.

To approximate the expectation in Eq. (11), we resort to a short-run MCMC-based approach, as typically done in training of EBMs (Song and Kingma, 2021) and LEBMs (Pang et al., 2020). For each datapoint, we generate approximate prior samples using a short-run Unadjusted Langevin Algorithm (ULA) chain targeting the prior distribution p_α . Specifically, for each data point y_m and a fixed parameter value α_k , we initialise the chain at $\hat{X}_{k,0}^m \sim p_0$, where $p_0 = \mathcal{N}(0, 1)$ is a standard Normal distribution, and evolve it for a fixed number of steps J with a step-size $\gamma > 0$:

$$\hat{X}_{k,j+1}^m = \hat{X}_{k,j}^m - \gamma \nabla_x U_{\alpha_k}(\hat{X}_{k,j}^m) + \sqrt{2\gamma} W_j^m, \quad (14)$$

where $(W_{k,j}^m)_{j,k \geq 0}$ for $m \in \{1, \dots, M\}$ denote standard d_x -dimensional Gaussian random variables. Then for every $k \geq 0$ and for each data-point y_m , we run an MCMC chain for J steps and we obtain the following system of equations

$$\tilde{\alpha}_{k+1} = \tilde{\alpha}_k - \frac{h}{MN} \sum_{n=1}^N \sum_{m=1}^M \nabla_\alpha U_{\tilde{\alpha}_k}(\tilde{X}_k^{m,n}) + \frac{h}{M} \sum_{m=1}^M \nabla_\alpha U_{\tilde{\alpha}_k}(\hat{X}_{k,J}^m) + \sqrt{\frac{2h}{MN}} \tilde{W}_k^\alpha, \quad (15)$$

$$\tilde{\beta}_{k+1} = \tilde{\beta}_k - \frac{h}{MN} \sum_{n=1}^N \sum_{m=1}^M \nabla_\beta V_{\tilde{\beta}_k}(\tilde{X}_k^{m,n}, y_m) + \sqrt{\frac{2h}{MN}} \tilde{W}_k^\beta, \quad (16)$$

$$\tilde{X}_{k+1}^{m,n} = \tilde{X}_k^{m,n} - h \nabla_x U_{\tilde{\alpha}_k}(\tilde{X}_k^{m,n}) - h \nabla_x V_{\tilde{\beta}_k}(\tilde{X}_k^{m,n}, y_m) + \sqrt{2h} \tilde{W}_k^{m,n}, \quad (17)$$

where $(\tilde{W}_k^\alpha)_{k \geq 0}$, $(\tilde{W}_k^\beta)_{k \geq 0}$, and $(\tilde{W}_k^{m,n})_{k \geq 0}$ denote independent standard Gaussian random variables of appropriate dimension. The complete algorithm is summarised in Algorithm 1.

3.2 Practical Implementation Details

In practice, we use several standard techniques to ensure stable and efficient training. (for details see Appendix C.1). To optimise the parameters (α, β) we use the Adam optimiser (Kingma and Ba, 2014), which uses adaptive step sizes and momentum, and has become the standard choice for training deep models due to its robustness across different scales of parameters. To handle large datasets efficiently, we rely on mini-batching: instead of using the full dataset at each iteration, we approximate the gradients using randomly sampled subsets of data (Robbins and Monroe, 1951). This reduces computational cost while still providing an unbiased estimate of the true gradient, and the stochasticity introduced by mini-batching can also help escape shallow local minima. Finally, since mini-batching implies that the decoder’s parameters are updated per batch rather than per full dataset pass, we introduce a suitable noise addition scheme for the posterior particles to ensure consistency with the Euler–Maruyama discretisation. The complete algorithm and further details are provided in Appendix C.1.

Algorithm 1 Energy-Based Interacting Particle Langevin Algorithm (Full version)

Require:

```

 $\{y_m\}_{m=1}^M, M$  # Dataset and its size
 $K$  # Number of iterations
 $N$  # Particles per data point
 $J$  # Prior sampling steps
 $h > 0$  # Step-size for discretisation
 $\gamma > 0$  # Step-size for prior sampling
 $\tilde{\theta}_0 = (\tilde{\alpha}_0, \tilde{\beta}_0)$  # Initial parameter value
 $\{X_0^{m,n}\}_{m,n=1}^{M,N}$  # Initial particles

1: for  $k = 0$  to  $K - 1$  do
2:   Sample  $\hat{X}_{k,J}^m$  using  $J$  steps of (14) with  $\tilde{\alpha}_k$  for each  $m \in \{1, \dots, M\}$ .
3:   Update  $\tilde{\alpha}_{k+1}$  according to Eq. (15)
4:   Update  $\tilde{\beta}_{k+1}$  according to Eq. (16)
5:   for  $(m, n) \in \{1, \dots, M\} \times \{1, \dots, N\}$  do
6:     Update  $X_{k+1}^{m,n}$  according to Eq. (17)
7:   end for
8: end for

```

4 Nonasymptotic Analysis

In this section, we study convergence of EBIPLA to the global maximisers of the marginal log-likelihood under strong convexity and L -smoothness assumptions. We focus on how convergence depends on both the number of particles N and the number of data points M . We first consider the case where we assume we have access to the exact gradient $\nabla_\theta \ell_M$ and then handle the inexact MCMC setting where we only have access to a biased estimator of $\nabla_\theta \ell_M$.

4.1 Assumptions

We first assume the negative joint log-likelihood is strongly convex and L -smooth for every data point.

A1. (*Strong convexity*) Let $v = (\theta, x)$ and $v' = (\theta', x')$. We assume that there exists $\mu > 0$ such that

$$\langle \nabla \phi_y(v) - \nabla \phi_y(v'), v - v' \rangle \geq \mu \|v - v'\|^2$$

for all $y \in \mathbb{R}^{d_y}$ and $v, v' \in \mathbb{R}^{d_\theta} \times \mathbb{R}^{d_x}$.

Remark 1. Note that $\phi_{y_m}(x, \theta) = -\log p_\theta(x, y_m)$ is the negative joint log-likelihood, thus **A1** is a joint log-concavity assumption that holds for $p_\theta(x, y_m)$ for every m . This also implies that the marginal likelihood $p_\theta(y_m)$ is μ -strongly log-concave (in θ) by the Prekopa-Leindler inequality (Gardner, 2002, Theorem 7.1). This then implies that $\ell_M(\theta)$ is also μ -strongly concave and hence has a unique maximiser. \diamond

A2. (*L-smoothness*) Let $v = (\theta, x)$. We assume that there exists $L > 0$ such that

$$\|\nabla \phi_y(v) - \nabla \phi_y(v')\| \leq L \|v - v'\|$$

for all $y \in \mathbb{R}^{d_y}$ and $v, v' \in \mathbb{R}^{d_\theta} \times \mathbb{R}^{d_x}$

4.2 Convergence with exact gradient

We first analyse the simplified setting in Eqs. (9)–(10). In other words, we assume that, equivalently, in Eqs. (11)–(13), the expectation w.r.t. p_{α_k} is known. This allows us to isolate the core convergence behavior of the particle-based updates as can be seen below.

Theorem 1. Suppose **A1**, **A2** hold. Let θ_k be the parameter marginal generated by iterates (9)–(10) (equivalently, (11)–(13)), then given a step size $0 < h \leq 2/(\mu + L)$, the following holds

$$\mathbb{E} [\|\theta_k - \theta_\star\|^2]^{1/2} \leq (1 - \mu h)^k C_0 + C_1 h^{1/2} + \frac{C_2}{\sqrt{MN}},$$

where C_0 is an explicit constant that only depends on the initial law of the system and

$$C_1 = 1.65 \frac{L}{\mu} \sqrt{\frac{d_\theta + MN d_x}{MN}}, \quad C_2 = \sqrt{\frac{d_\theta}{\mu}},$$

and θ_\star denotes the unique maximiser of ℓ_M .

Proof. A full proof can be found in Appendix B.1. \square

Remark 2. Theorem 1 implies that, for sufficiently large N and k and sufficiently small h , the iterates of Eqs. (11)–(13) can be made arbitrarily close to θ_\star . More precisely for a fixed number of data points M and a target accuracy $\varepsilon > 0$ choosing $N = \mathcal{O}(\varepsilon^{-2} M^{-1} d_\theta)$ makes the last term of the bound in Theorem 1 of order $\mathcal{O}(\varepsilon)$. Next, setting $h = \mathcal{O}(\varepsilon^2 d_x^{-1})$ makes the middle term of order $\mathcal{O}(\varepsilon)$. Finally setting $k \geq \tilde{\mathcal{O}}(d_x \varepsilon^{-2})$ ensures that the first term is $\mathcal{O}(\varepsilon)$. With these choices, we obtain $\mathbb{E}[\|\theta_k - \theta_\star\|^2]^{1/2} \leq \mathcal{O}(\varepsilon)$. Note that since $N = \mathcal{O}(M^{-1} \varepsilon^{-2})$, for large datasets the bound can be made small with small N . \diamond

Below, we provide a sketch of the proof. We start by noting that $\mathbb{E}[\|\theta_n - \theta_\star\|^2]^{1/2} = W_2(\mathcal{L}(\theta_n), \delta_{\theta_\star})$ since δ_{θ_\star} is a Dirac measure (Santambrogio, 2015, Section 1.4). Then via an application of the triangle inequality, we obtain:

$$\mathbb{E} [\|\theta_n - \bar{\theta}_\star\|^2]^{1/2} = W_2(\mathcal{L}(\theta_n), \delta_{\bar{\theta}_\star}) \leq \underbrace{W_2(\pi_\Theta, \delta_{\bar{\theta}_\star})}_{\text{concentration}} + \underbrace{W_2(\mathcal{L}(\theta_n), \pi_\Theta)}_{\text{convergence}}.$$

We establish concentration using Altschuler and Chewi (2024, Lemma A.8) and convergence by adapting Dalalyan and Karagulyan (2019, Theorem 1) for our system.

4.3 Convergence with inexact gradient

Since the expectation with respect to the prior cannot be computed exactly, the gradient update in Eq. (11) is not directly available. To address this, we approximate the expectation using a ULA chain, which yields a biased estimator of $\mathbb{E}_{p_{\alpha_k}(x)}[\nabla_\alpha U_{\alpha_k}(x)]$ at each iteration. Following Dalalyan and Karagulyan (2019), we impose the assumptions below to control the bias introduced by this approximation and the variance of the deviation from the true quantity.

Let $g_k := (1/M) \sum_{m=1}^M \nabla_\alpha U_{\alpha_k}(\hat{X}_{k,J}^m)$ as defined in Eq. (15). Let $\zeta_k := \mathbb{E}_{p_{\alpha_k}(x)}[\nabla_\alpha U_{\alpha_k}(x)] - g_k$ for all $k \in \{1, \dots, K\}$. Finally, let \mathcal{F}_k be the σ -algebra generated by the algorithm (15)–(17) up to iteration k .

A3. There exist $\delta > 0$ and $\sigma > 0$ such that

$$\mathbb{E} [\|\mathbb{E}[\zeta_k | \mathcal{F}_k]\|^2] \leq \delta^2, \quad \mathbb{E} [\|\zeta_k - \mathbb{E}[\zeta_k | \mathcal{F}_k]\|^2] \leq \sigma^2$$

for $k \geq 0$, where \tilde{W}_{k+1}^α , \tilde{W}_{k+1}^β , $\tilde{W}_{k+1}^{m,n}$ for all $m \in \{1, \dots, M\}$, $n \in \{1, \dots, N\}$ in Eqs. (15)–(17) are independent of $(\zeta_0, \dots, \zeta_k)$.

Intuitively, the bias ζ_k arises from a finite run of ULA. It is possible to reduce this bias by increasing the number of prior iterations in our setting. In this setting we can get a similar bound as in Theorem 1 with additional terms arising from the bias in the expectation estimate.

Theorem 2. Suppose **A1**, **A2**, **A3** hold. Let $\tilde{\theta}_k = (\tilde{\alpha}_k, \tilde{\beta}_k)$ be the parameter marginal generated by iterates (15)–(17), then given a step size $0 < h \leq 2/(\mu + L)$, the following holds

$$\mathbb{E} \left[\|\tilde{\theta}_k - \theta_\star\|^2 \right]^{1/2} \leq (1 - \mu h)^k \tilde{C}_0 + \tilde{C}_1 h^{1/2} + \frac{\tilde{C}_2}{\sqrt{MN}},$$

where \tilde{C}_0 is a fully explicit constant that only depends on the initial law of the system and

$$\begin{aligned} \tilde{C}_1 &= 1.65 \left(\frac{L}{\mu} \right) \sqrt{\frac{d_\theta + MN d_x}{MN}} + \frac{\sigma^2}{1.65 L (MN)^{3/2} \sqrt{d_\theta + MN d_x} + \sigma MN \sqrt{\mu}}, \\ \tilde{C}_2 &= \frac{\delta}{\mu} + \sqrt{\frac{d_\theta}{\mu}}. \end{aligned}$$

Proof. See Appendix B.3 for the proof. \square

Remark 3. While we hide the dimension dependence of δ and σ , in practice, they will depend on d_α as the gradient error mainly arises in the α component. Also, we note $\delta := \delta(J)$ depends on the number of ULA iterations J and decreases as J increases. Furthermore, if the ULA chain is stable, geometrically ergodic, and γ is sufficiently small so that the bias introduced from inexactly targeting p_α can be controlled, this is a sensible assumption. \diamond

5 Related Works

Training EBMs. Efficient training of EBMs remains a fundamental challenge in generative modelling. As an approximation to MLE, Hinton (2002) proposed Contrastive Divergence (CD) to estimate the gradients of EBM using non-convergent MCMC chains started from the data points. This was subsequently improved Persistent Contrastive Divergence (PCD), which initialises the chain for the current iteration from the final state of the chain in the previous iteration (Tieleman, 2008). However, CD with short run MCMC introduces uncontrolled bias in the estimation of the energy function (Nijkamp et al., 2020). To mitigate this bias, Carbone et al. (2024) developed training algorithms using Jarzynski’s equality from non-equilibrium thermodynamics. Schröder et al. (2023, 2024) introduce the Energy Discrepancy loss that bypasses MCMC sampling. More recently, Oliva et al. (2025) introduced a continuous-time formulation of PCD, deriving explicit bounds on the error between PCD iterates and the MLE solution, and use it to introduce an efficient training algorithm for EBMs.

EBMs in the Latent Space. Since training EBMs in the ambient space can be expensive, Pang et al. (2020) propose a latent space formulation where the prior is modelled by an EBM, and the latent variables are decoded into the ambient space using a simple Gaussian decoder. This approach is later refined using diffusion-amortised MCMC (Yu et al., 2023). Instead of joint learning of the EBM prior with the generator, Xiao et al. (2021) train an EBM in the latent space of a pre-trained VAE. Furthermore, Xiao and Han (2022) suggest to use a multi-stage noise contrastive estimation to learn the energy-based prior. Recently, Yuan et al. (2025) extend those approaches to multimodal settings, introducing a variational learning scheme for the generator posterior combined with an energy-based prior.

Interacting Particle Algorithms for Learning. Kuntz et al. (2023) introduce Particle Gradient Descent (PGD), a diffusion-based particle algorithm for MMLE in latent variable models that jointly optimises model parameters and samples from the posterior distribution of the latent variables. Building on this framework, Akyildiz et al. (2025) incorporate additive noise in the parameter updates and establish associated non-asymptotic convergence guarantees. The theoretical guarantees for PGD is established in Caprio et al. (2025). Since then, particle-based learning methods have been taking off

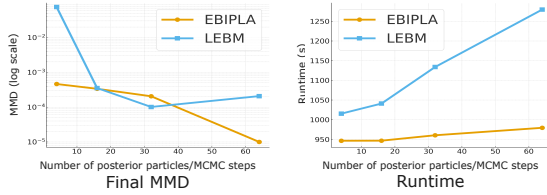


Figure 1: Comparison of MMD (left) and runtime (right) for increasing numbers of posterior particles (EBIPLA) or MCMC steps (LEBM) trained on the rotated Swiss roll dataset.

in various directions, see e.g. [Lim et al. \(2024\)](#); [Oliva and Akyildiz \(2024\)](#) for momentum-enriched variants, [Encinar et al. \(2025\)](#) for extensions to non-smooth settings, [Glyn-Davies et al. \(2025\)](#) for applications to inverse problems.

6 Experiments

To evaluate the generative performance of EBIPLA we train it on a synthetic dataset (Section 6.1) and on three image datasets (Section 6.2). On the synthetic task we benchmark against the closest baseline, LEBM ([Pang et al., 2020](#)). Compared to the benchmark across both settings, EBIPLA attains slightly better generative performance while delivering substantially lower runtime at matched compute budgets. For the image datasets, we additionally compare to other LVMs.

6.1 Synthetic datasets

We evaluate EBIPLA on a synthetic rotated Swiss roll dataset. More precisely, we generate a Swiss roll in a 2-dimensional latent space \mathbb{R}^2 and then map it to the ambient space through an orthogonal transformation $T : \mathbb{R}^2 \rightarrow \mathbb{R}^2$. (for details see App. D.1)

To contextualize our results, we consider the closest baseline, LEBM, for comparison. For both models we use 500 prior iterations and matched posterior computational budgets of $N \in \{4, 16, 32, 64\}$, where N denotes the number of posterior particles (EBIPLA) and for or posterior MCMC steps (LEBM). We train both models for 200 epochs and report the final-epoch Maximum Mean Discrepancy (MMD) estimate ([Gretton et al., 2012](#)) between the generated and the true samples, alongside wall-clock runtime, each averaged over 20 runs. (for hyperparameter details see Appendix D.1) Figure 1 shows that EBIPLA achieves lower MMD for nearly all particle counts, with performance remaining comparable at $N = 8, 16$. EBIPLA is much faster: its runtime grows sub-linearly with particle count, whereas LEBM’s runtime increases approximately linearly with iteration count (Fig. 1). Notably, even at the largest investigated particle count, our method remains faster than LEBM run with the smallest investigated number of posterior iterations. Furthermore, we can see in Figure 2 that the sample quality as well as the accuracy of the learned energy landscape improves with increasing number of posterior particles/iterations. EBIPLA performs comparably in terms of sample quality to LEBM, however learns the energy landscape more accurately.

6.2 Images

To validate the effectiveness of our method on high dimensional data, we train EBIPLA on three standard image datasets: CIFAR10 ([Krizhevsky and Hinton, 2009](#)), SVHN ([Netzer et al., 2011](#)), and CelebA64 ([Liu et al., 2015](#)). Following [Pang et al. \(2020\)](#), we use the same architecture for both the

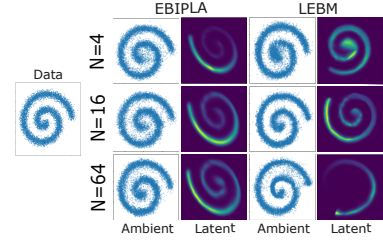
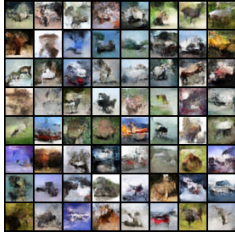
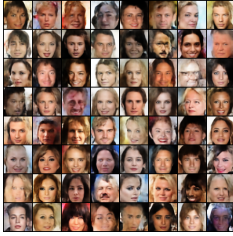


Figure 2: Samples generated with EBIPLA and LEBM trained on the rotated Swiss roll dataset for increasing numbers of posterior particles (or MCMC steps) with energy landscapes.



(a) CIFAR-10



(b) CelebA64



(c) SVHN

| No. of Particles | FID |
|------------------|-------|
| $N = 1$ | 31.49 |
| $N = 4$ | 28.12 |
| $N = 16$ | 27.37 |
| $N = 32$ | 26.74 |

(d) Effect of the no. of posterior particles on the generation performance of EBIPLA trained on SVHN.

Figure 3: Samples generated with EBIPLA trained on CIFAR-10, CelebA64, and SVHN.

Table 1: Comparison of $\text{MSE}(\downarrow)$ and $\text{FID}(\downarrow)$ on the SVHN, CIFAR-10, and CelebA64 datasets.

| Model | SVHN | | CIFAR-10 | | CelebA | |
|---------------------------------|--------------|--------------|--------------|--------|--------------|--------------|
| | MSE | FID | MSE | FID | MSE | FID |
| VAE (Kingma and Welling, 2014) | 0.019 | 46.78 | 0.057 | 106.37 | 0.021 | 65.75 |
| LEBM (Pang et al., 2020) | 0.008 | 29.44 | 0.020 | 70.15 | 0.013 | 37.87 |
| ED-LEBM (Schröder et al., 2023) | 0.006 | 28.10 | 0.023 | 73.58 | 0.009 | 36.73 |
| EBIPLA (ours) | 0.005 | 27.59 | 0.020 | 79.64 | 0.014 | 34.71 |

energy-based prior and the generator network. We train all models for 200 epochs with a batch size of 128; the number of particles is set to $N = 10$ to balance performance and efficiency following Kuntz et al. (2023). The complete implementation details and training hyperparameters are provided in Section D.2.

Generation and Reconstruction. We evaluate the generative performance of our model quantitatively with the Fréchet Inception Distance (FID) (Heusel et al., 2017) using 50,000 samples generated by the energy-based prior and decoded back to the pixel space. Additionally, we measure the reconstruction quality in terms of mean-squared error (MSE) on the validation set. We obtain the reconstructions as the maximum a posteriori (MAP) estimates of $p_\theta(x|y)$ (cf. Section 3) following the implementation in Kuntz et al. (2023); we provide further details of the evaluation procedure in Section D.2. In Table 1, we show that our EBIPLA achieves comparable performance among relevant baselines. We also remark that EBIPLA has much shorter runtimes compared to LEBM (Pang et al., 2020) across settings due to its efficient formulation. Furthermore, we show on the SVHN dataset that the performance of EBIPLA improves as we increase the number of posterior particles used in Table 3d, aligning with our results on the synthetic data and empirically validating our theoretical results.

Latent Representations. To qualitatively assess the learned representations, we visualize interpolations in the latent space. We linearly interpolate between the latent vectors x_0 and x_1 as $\text{lerp}(x_0, x_1, t) = tx_0 + (1 - t)x_1$; we then decode those interpolants back to the pixel space using the trained generator. For training images, we select index m and extract one of the posterior particles randomly from the N particles $X_K^{m,1:N}$ obtained from training (cf. Algorithm 1); for validation

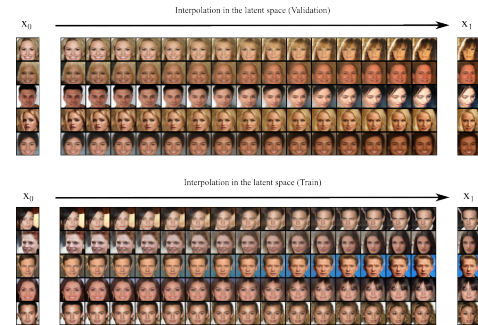


Figure 4: Latent space interpolation of EBIPLA on the training (bottom) and validation set (top).

images, we use the MAP estimate as in our reconstruction experiments. Figure 4 shows the resulting interpolation trajectories, which suggests that EBIPLA has learned a smooth and semantically meaningful latent space.

7 Conclusion

Motivated by recent advances in particle-based training methods, we propose an interacting particle method for learning latent energy-based models (EBIPLA). By discretising a system of SDEs that is designed to admit an invariant measure concentrating around the maximiser of the marginal log-likelihood, we obtain a practical algorithm that is both scalable and theoretically grounded (Section 3). In Section 4, we provide to the best of our knowledge the first convergence bounds for training latent energy-based models under the strong log-concavity and smoothness assumptions. In particular, we show that the algorithm converges to the optimal parameters with increasing number of both data points and particles; this ensures that even with a small number of particles reliable performance can be achieved on large datasets. (Theorem 1, Theorem 2). Although the convergence bounds are obtained under the strong log-concavity we expect those can be further relaxed using similar ideas to Zhang et al. (2023). The experiments on both synthetic and image data show that EBIPLA achieves competitive generative and reconstructive performance among relevant baselines (Section 6).

Lastly, while for fairness of comparison we use a simple Langevin chain to approximate the prior expectation, the framework is agnostic to the choice of sampler: more advanced samplers such as Hamiltonian Monte Carlo (HMC) (Duane et al., 1987), NUTS (Hoffman et al., 2014) or Riemann manifold adjusted version of HMC (Girolami and Calderhead, 2011) could be employed to improve the generative performance. In addition, extensions to underdamped settings offers a promising direction to obtain accelerated versions of EBIPLA with theoretical guarantees (Oliva and Akyildiz, 2024).

Acknowledgements

J. M. is supported by EPSRC through the Modern Statistics and Statistical Machine Learning (StatML) CDT programme, grant no. EP/S023151/1. T. W. is supported by the Roth Scholarship from the Department of Mathematics, Imperial College London.

References

Akyildiz, O. D., Crucinio, F. R., Girolami, M., Johnston, T., and Sabanis, S. (2025). Interacting particle Langevin algorithm for maximum marginal likelihood estimation. *ESAIM: Probability and Statistics*, 29:243–280.

Altschuler, J. M. and Chewi, S. (2024). Faster high-accuracy log-concave sampling via algorithmic warm starts. *Journal of the ACM*, 71(3):1–55.

Atchadé, Y., Jiang, K., and Sun, Y. (2023). On generative energy-based models. Manuscript.

Bengio, Y., Courville, A., and Vincent, P. (2013). Representation learning: A review and new perspectives. *IEEE transactions on pattern analysis and machine intelligence*, 35(8):1798–1828.

Caprio, R., Kuntz, J., Power, S., and Johansen, A. M. (2025). Error bounds for particle gradient descent, and extensions of the log-Sobolev and Talagrand inequalities. *Journal of Machine Learning Research*, 26(103):1–38.

Carbone, D., Hua, M., Coste, S., and Vanden-Eijnden, E. (2024). Efficient training of energy-based models using Jarzynski equality. *Journal of Statistical Mechanics: Theory and Experiment*, 2024(10):104019.

Dalalyan, A. S. and Karagulyan, A. (2019). User-friendly guarantees for the Langevin Monte Carlo with inaccurate gradient. *Stochastic Processes and their Applications*, 129(12):5278–5311.

De Bortoli, V., Durmus, A., Pereyra, M., and Vidal, A. F. (2021). Efficient stochastic optimisation by unadjusted Langevin Monte Carlo. *Statistics and Computing*, 31(3):29.

Dempster, A. P., Laird, N. M., and Rubin, D. B. (1977). Maximum likelihood from incomplete data via the EM algorithm. *Journal of the royal statistical society: series B (methodological)*, 39(1):1–22.

Deng, Y., Bakhtin, A., Ott, M., Szlam, A., and Ranzato, M. (2021). Residual energy-based models for text generation. *Journal of Machine Learning Research*, 22:1–41.

Douc, R., Moulines, E., and Stoffer, D. (2014). *Nonlinear time series: Theory, methods and applications with R examples*. CRC press.

Du, Y., Durkan, C., Strudel, R., Tenenbaum, J. B., Dieleman, S., Fergus, R., Sohl-Dickstein, J., Doucet, A., and Grathwohl, W. S. (2023). Reduce, reuse, recycle: Compositional generation with energy-based diffusion models and mcmc. In *International conference on machine learning*, pages 8489–8510. PMLR.

Du, Y., Li, S., and Mordatch, I. (2020). Compositional visual generation with energy based models. In *Advances in Neural Information Processing Systems*.

Du, Y. and Mordatch, I. (2019). Implicit generation and modeling with energy based models. *Advances in neural information processing systems*, 32.

Duane, S., Kennedy, A. D., Pendleton, B. J., and Roweth, D. (1987). Hybrid monte carlo. *Physics letters B*, 195(2):216–222.

Encinar, P. C., Crucinio, F. R., and Akyildiz, O. D. (2025). Proximal interacting particle Langevin algorithms. In *The 41st Conference on Uncertainty in Artificial Intelligence*.

Gardner, R. (2002). The brunn-minkowski inequality. *Bulletin of the American mathematical society*, 39(3):355–405.

Girolami, M. and Calderhead, B. (2011). Riemann manifold langevin and hamiltonian monte carlo methods. *Journal of the Royal Statistical Society Series B: Statistical Methodology*, 73(2):123–214.

Gladstone, A., Nanduru, G., Islam, M. M., Han, P., Ha, H., Chadha, A., Du, Y., Ji, H., Li, J., and Iqbal, T. (2025). Energy-based transformers are scalable learners and thinkers. *arXiv preprint arXiv:2507.02092*.

Glaser, P., Arbel, M., Doucet, A., and Gretton, A. (2022). Maximum likelihood learning of energy-based models for simulation-based inference. *arXiv preprint arXiv:2210.14756*.

Glyn-Davies, A., Duffin, C., Kazlauskaitė, I., Girolami, M., and Akyildiz, Ö. D. (2025). Statistical finite elements via interacting particle Langevin dynamics. *SIAM/ASA Journal on Uncertainty Quantification*, 13(3):1200–1227.

Grathwohl, W., Wang, K.-C., Jacobsen, J.-H., Duvenaud, D., Norouzi, M., and Swersky, K. (2020). Your classifier is secretly an energy based model and you should treat it like one. In *International Conference on Learning Representations*.

Gretton, A., Borgwardt, K. M., Rasch, M. J., Schölkopf, B., and Smola, A. J. (2012). A kernel two-sample test. *Journal of Machine Learning Research*, 13(25):723–773.

Heusel, M., Ramsauer, H., Unterthiner, T., Nessler, B., and Hochreiter, S. (2017). GANs trained by a two time-scale update rule converge to a local nash equilibrium. In Guyon, I., Luxburg, U. V., Bengio, S., Wallach, H., Fergus, R., Vishwanathan, S., and Garnett, R., editors, *Advances in Neural Information Processing Systems*, volume 30. Curran Associates, Inc.

Hinton, G. E. (2002). Training products of experts by minimizing contrastive divergence. *Neural computation*, 14(8):1771–1800.

Hoffman, M. D., Gelman, A., et al. (2014). The No-U-Turn sampler: adaptively setting path lengths in Hamiltonian Monte Carlo. *J. Mach. Learn. Res.*, 15(1):1593–1623.

Hwang, C.-R. (1980). Laplace’s method revisited: weak convergence of probability measures. *The Annals of Probability*, pages 1177–1182.

Kingma, D. and Ba, J. (2014). Adam: A method for stochastic optimization. *International Conference on Learning Representations*.

Kingma, D. P. and Welling, M. (2014). Auto-encoding variational bayes. *2nd International Conference on Learning Representations, ICLR*.

Krizhevsky, A. and Hinton, G. (2009). Learning multiple layers of features from tiny images. Technical Report 0, University of Toronto, Toronto, Ontario.

Kuntz, J., Lim, J. N., and Johansen, A. M. (2023). Particle algorithms for maximum likelihood training of latent variable models. In *International Conference on Artificial Intelligence and Statistics*, pages 5134–5180. PMLR.

Lim, J. N., Kuntz, J., Power, S., and Johansen, A. M. (2024). Momentum particle maximum likelihood. In *Proceedings of the Forty-First International Conference on Machine Learning*.

Liu, Z., Luo, P., Wang, X., and Tang, X. (2015). Deep learning face attributes in the wild. In *Proceedings of International Conference on Computer Vision (ICCV)*.

Loaiza-Ganem, G., Ross, B. L., Hosseinzadeh, R., Caterini, A. L., and Cresswell, J. C. (2024). Deep generative models through the lens of the manifold hypothesis: A survey and new connections. *arXiv preprint arXiv:2404.02954*.

Netzer, Y., Wang, T., Coates, A., Bissacco, A., Wu, B., and Ng, A. Y. (2011). Reading digits in natural images with unsupervised feature learning. In *NIPS Workshop on Deep Learning and Unsupervised Feature Learning 2011*.

Nijkamp, E., Hill, M., Han, T., Zhu, S.-C., and Wu, Y. N. (2020). On the anatomy of MCMC-based maximum likelihood learning of energy-based models. In *Proceedings of the AAAI Conference on Artificial Intelligence*, volume 34, pages 5272–5280. AAAI Press.

Oliva, P. F. V. and Akyildiz, O. D. (2024). Kinetic interacting particle langevin Monte Carlo. *arXiv preprint arXiv:2407.05790*.

Oliva, P. F. V., Akyildiz, O. D., and Duncan, A. (2025). Uniform-in-time convergence bounds for persistent contrastive divergence algorithms.

Pang, B., Han, T., Nijkamp, E., Zhu, S.-C., and Wu, Y. N. (2020). Learning latent space energy-based prior model. *Advances in Neural Information Processing Systems*, 33:21994–22008.

Raginsky, M., Rakhlin, A., and Telgarsky, M. (2017). Non-convex learning via stochastic gradient Langevin dynamics: a nonasymptotic analysis. In *Conference on Learning Theory*, pages 1674–1703. PMLR.

Robbins, H. and Monro, S. (1951). A stochastic approximation method. *The annals of mathematical statistics*, pages 400–407.

Santambrogio, F. (2015). *Optimal transport for applied mathematicians*. Springer.

Schröder, T., Ou, Z., Li, Y., and Duncan, A. B. (2024). Energy-based modelling for discrete and mixed data via heat equations on structured spaces. In *The Thirty-eighth Annual Conference on Neural Information Processing Systems*.

Schröder, T., Ou, Z., Lim, J. N., Li, Y., Vollmer, S. J., and Duncan, A. (2023). Energy discrepancies: A score-independent loss for energy-based models. In *Thirty-seventh Conference on Neural Information Processing Systems*.

Song, Y. and Kingma, D. P. (2021). How to train your energy-based models. *arXiv preprint arXiv:2101.03288*.

Song, Y., Sohl-Dickstein, J., Kingma, D. P., Kumar, A., Ermon, S., and Poole, B. (2021). Score-based generative modeling through stochastic differential equations. In *International Conference on Learning Representations*.

Tieleman, T. (2008). Training restricted Boltzmann machines using approximations to the likelihood gradient. In *Proceedings of the 25th international conference on Machine learning*, pages 1064–1071.

Wang, T. Y., Kuntz, J., and Akyildiz, O. D. (2025). Training latent diffusion models with interacting particle algorithms. *arXiv preprint arXiv:2505.12412*.

Whiteley, N., Gray, A., and Rubin-Delanchy, P. (2025). Statistical exploration of the manifold hypothesis. *Journal of the Royal Statistical Society: Series B*.

Xiao, Z. and Han, T. (2022). Adaptive multi-stage density ratio estimation for learning latent space energy-based model. In *Advances in Neural Information Processing Systems*.

Xiao, Z., Kreis, K., Kautz, J., and Vahdat, A. (2021). {VAEBM}: A symbiosis between variational autoencoders and energy-based models. In *International Conference on Learning Representations*.

Yu, P., Zhu, Y., Xie, S., Ma, X., Gao, R., Zhu, S.-C., and Wu, Y. N. (2023). Learning energy-based prior model with diffusion-amortized MCMC. In *Thirty-seventh Conference on Neural Information Processing Systems*.

Yuan, S., Cui, J., Li, H., and Han, T. (2025). Learning multimodal latent generative models with energy-based prior. In Leonardis, A., Ricci, E., Roth, S., Russakovsky, O., Sattler, T., and Varol, G., editors, *Computer Vision – ECCV 2024*, pages 86–100, Cham. Springer Nature Switzerland.

Zhai, S., Cheng, Y., Lu, W., and Zhang, Z. (2016). Deep structured energy based models for anomaly detection. In *Proceedings of the 33rd International Conference on Machine Learning (ICML)*, pages 1100–1109. PMLR.

Zhang, Y., Akyildiz, Ö. D., Damoulas, T., and Sabanis, S. (2023). Nonasymptotic estimates for stochastic gradient Langevin dynamics under local conditions in nonconvex optimization. *Applied Mathematics & Optimization*, 87(2):25.

Appendix

A Preliminary results

Recall given a data point y that we define $p_\theta(x, y) = p_\alpha(x)p_\beta(y, x)$ and recall our notation $\phi_y(\theta, x)$ as:

$$\phi_y(x, \theta) = -\log p_\theta(x, y). \quad (18)$$

We can write the gradient:

$$\nabla_\theta \log p_\theta(x, y) = \nabla_\theta \log p_\alpha(x) + \nabla_\theta \log p_\beta(y|x). \quad (19)$$

A.1 Derivation of $\nabla_\alpha \phi_y(\theta, x)$

Since $p_\beta(y_m|x)$ is independent of α the gradient reads

$$\nabla_\alpha \phi_y(\theta, x) = -\nabla_\alpha \log p_\theta(x, y) = -\nabla_\alpha \log p_\alpha(x). \quad (20)$$

By definition $p_\alpha(x) = e^{-U_\alpha(x)}/Z_\alpha$ so

$$\nabla_\alpha \phi_y(\theta, x) = -\nabla_\alpha \log p_\alpha(x) = \nabla_\alpha U_\alpha(x) + \nabla_\alpha \log Z_\alpha \quad (21)$$

where $Z_\alpha = \int e^{-U_\alpha(x)}dx$ is the normalising constant which is unknown. However, the gradient of $\log Z_\alpha$ can be rewritten as

$$\nabla_\alpha \log Z_\alpha = \frac{\nabla_\alpha Z_\alpha}{Z_\alpha} = \frac{\int \nabla_\alpha e^{-U_\alpha(x)}dx}{Z_\alpha} \quad (22)$$

$$= - \int \nabla_\alpha U_\alpha(x)p_\alpha(x)dx = -\mathbb{E}_{p_\alpha(x)}[\nabla_\alpha U_\alpha(x)] \quad (23)$$

hence

$$\nabla_\alpha \phi_y(\theta, x) = \nabla_\alpha U_\alpha(x) - \mathbb{E}_{p_\alpha(x)}[\nabla_\alpha U_\alpha(x)] \quad (24)$$

and for a set of particles $\{X_t^{m,n}\}_{m=1,n=1}^{M,N}$ and a parameter $\theta_k = (\alpha_k, \beta_k)$

$$\frac{1}{MN} \sum_{m=1}^M \sum_{n=1}^N \nabla_\alpha \phi_{y_m}(\theta_k, X_k^{m,n}) = \frac{1}{MN} \sum_{m=1}^M \sum_{n=1}^N \nabla_\alpha U_{\alpha_k}(X_t^{m,n}) - \mathbb{E}_{p_{\alpha_k}(x)}[\nabla_\alpha U_{\alpha_k}(x)] \quad (25)$$

A.2 Derivation of $\nabla_\beta \phi_y(\theta, x)$

Similarly, given a data point y since $p_\alpha(x)$ is independent of β the gradient of $\phi_y(\theta, x)$ with respect to β reads

$$\nabla_\beta \phi_y(\theta, x) = -\nabla_\beta \log p_\theta(x, y) = -\nabla_\beta \log p_\beta(y|x) \quad (26)$$

Let $V_\beta(y, x_m) = -\log p_\beta(y|x)$ then for a set of particles $\{X_t^{m,n}\}_{m=1,n=1}^{M,N}$ and a parameter $\theta_k = (\alpha_k, \beta_k)$

$$\frac{1}{MN} \sum_{m=1}^M \sum_{n=1}^N \nabla_\beta \phi_{y_m}(\theta_k, X_k^{m,n}) = \frac{1}{MN} \sum_{m=1}^M \sum_{n=1}^N \nabla_\beta V_\beta(y_m, X_t^{m,n}) \quad (27)$$

which, if we assume a standard isotropic Gaussian decoder i.e. $p(y_m|x) \sim N(g_\beta(x), \sigma)$ then $V_\beta(y_m, x) = \frac{\|y_m - g_\beta(x)\|^2}{2\sigma^2} + \text{const}$ where g_β denotes the encoder.

A.3 Derivation of $\nabla_x \phi_y(\theta, x)$

Recall $V_\beta(x, y) = -\log p_\beta(y_m|x)$, then given a data point y , the gradient of $\phi_y(\theta, x)$ with respect to x reads

$$\nabla_x \phi_y(\theta, x) = -\nabla_x \log p_\theta(x, y) = -\nabla_x \log p_\alpha(x) - \nabla_x \log p_\beta(y|x) \quad (28)$$

$$= \nabla_x U_\alpha(x) + \nabla_x V_\beta(x, y) = \nabla_x U_\alpha(x) + \nabla_x V_\beta(x, y) \quad (29)$$

since the normalising constant Z_α is independent of x .

B Proofs

B.1 Proof of Theorem 1

Proof. Recall the system of SDEs defined in (9)–(10)

$$\theta_{k+1} = \theta_k - \frac{h}{MN} \sum_{m=1}^M \sum_{n=1}^N \nabla_1 \phi_{y_m}(\theta_k, X_k^{m,n}) + \sqrt{\frac{2h}{MN}} W_k, \quad (30)$$

$$X_{k+1}^{m,n} = X_k^{m,n} - h \nabla_2 \phi_{y_m}(\theta_k, X_k^{m,n}) + \sqrt{2h} W_k^{m,n}, \quad (31)$$

where $\phi_{y_m}(\theta, x) = -\log p_\theta(x, y_m)$ and which is equivalent to the SDE system in (11)–(13). In the above display, we use ∇_1 and ∇_2 to denote the derivatives w.r.t. first and second arguments of ϕ_{y_m} , respectively, as this will be important in the proof.

Consider the function $\Phi : \mathbb{R}^{d_\theta} \times (\mathbb{R}^{d_x})^{M \times N} \rightarrow \mathbb{R}$, defined as

$$\Phi(\theta, z^{1:M, 1:N}) = \sum_{m=1}^M \sum_{n=1}^N \phi_{y_m}(\theta, \sqrt{MN} z^{m,n}).$$

Next, let us define the following probability distribution:

$$\pi(\theta, z^{1:M, 1:N}) \propto \exp(-\Phi(\theta, z^{1:M, 1:N})).$$

Our strategy in this proof is to notice that the iterates (30)–(31) can be seen as a discretisation of an SDE, targeting π . In order to see this, consider the Langevin SDE targeting π :

$$d\theta_t = - \sum_{m=1}^M \sum_{n=1}^N \nabla_1 \phi_{y_m}(\theta_t, \sqrt{MN} Z_t^{m,n}) dt + \sqrt{2} dB_t, \quad (32)$$

$$dZ_t^{m,n} = -\sqrt{MN} \nabla_2 \phi_{y_m}(\theta_t, \sqrt{MN} Z_t^{m,n}) dt + \sqrt{2} dB_t^{m,n}. \quad (33)$$

Euler-Maruyama discretisation of this SDE with step-size $\bar{h} = h/MN$ gives us

$$\theta_{k+1} = \theta_k - \frac{h}{MN} \sum_{m=1}^M \sum_{n=1}^N \nabla_1 \phi_{y_m}(\theta_k, \sqrt{MN} Z_k^{m,n}) + \sqrt{\frac{2h}{MN}} W_k, \quad (34)$$

$$Z_{k+1}^{m,n} = Z_k^{m,n} - \frac{h}{\sqrt{MN}} \nabla_2 \phi_{y_m}(\theta_k, \sqrt{MN} Z_k^{m,n}) + \sqrt{\frac{2h}{MN}} W_k^{m,n}. \quad (35)$$

Now, if we define $X_k^{m,n} = \sqrt{MN} Z_k^{m,n}$, we recover exactly (9)–(10) (i.e. (30)–(31) above). In other words, up to a simple rescaling, the systems are identical. Most importantly, θ -marginals of both scaled algorithms are identical, thus the analysis of the iterates defined in (34) will give us the convergence of the parameters.

To assess first whether this target distribution is desirable, we consider the θ -marginal of π , denoted by π_Θ . That is, π_Θ is obtained by integrating out all latent variables $z^{1:M,1:N}$ from the joint distribution π :

$$\begin{aligned}
\pi_\Theta(\theta) &= \int \pi(\theta, z^{1:M,1:N}) dz^{1:M,1:N} = \int \exp(-\Phi(\theta, z^{1:M,1:N})) dz^{1:M,1:N} \\
&= \int \prod_{m=1}^M \prod_{n=1}^N \exp(-\phi_{y_m}(\theta, \sqrt{MN} z^{m,n})) dz^{1:M,1:N} = \prod_{m=1}^M \prod_{n=1}^N \int \exp(-\phi_{y_m}(\theta, \sqrt{MN} z^{m,n})) dz^{m,n}, \\
&\propto \prod_{m=1}^M \left(\int \exp(-\phi_{y_m}(\theta, x)) dx \right)^N \propto \prod_{m=1}^M p_\theta(y_m)^N, \\
&\propto \exp \left(N \sum_{m=1}^M \log p_\theta(y_m) \right).
\end{aligned}$$

In other words, as $N \rightarrow \infty$, $\pi_\Theta(\theta)$ concentrates around the maximisers of the loss we would like to optimise (i.e. ℓ_M).

Next, we look at the rate of convergence. To proceed, we first establish the convexity properties of the function Φ . Under **A1** and **A2**, ϕ_{y_m} is μ -strongly convex and L -smooth in both arguments for all $m \in \{1, \dots, M\}$. By arguments analogous to those in [Oliva and Akyildiz \(2024, Lemmas A.4–A.5\)](#), it follows that Φ is $MN\mu$ -strongly convex and MNL -smooth in both arguments. This means that an exponential convergence rate will hold by using well-known convergence results of Langevin diffusions. Let $\nu_k = \mathcal{L}(\theta_k, Z_k^{1:M,1:N})$ be the law of the system in (34)–(35). Given that, the target π is $\bar{\mu} = MN\mu$ -strongly log-concave and $\bar{L} = MNL$ log-smooth, the discretisation of this system with $\bar{h} = h/MN$ satisfies [\(Dalalyan and Karagulyan, 2019, Theorem 1\)](#)

$$W_2(\nu_k, \pi) \leq (1 - \bar{h}\bar{\mu})^k W_2(\nu_0, \pi) + 1.65 \left(\frac{\bar{L}}{\bar{\mu}} \right) \sqrt{d_\theta + MN d_x} \bar{h}^{1/2}, \quad (36)$$

where $0 < \bar{h} \leq 2/(\bar{\mu} + \bar{L})$. Plugging $\bar{h} = h/MN$, $\bar{\mu} = MN\mu$, and $\bar{L} = MNL$ to the above bound, we get

$$W_2(\nu_k, \pi) \leq (1 - h\mu)^k W_2(\nu_0, \pi) + 1.65 \left(\frac{L}{\mu} \right) \sqrt{\frac{d_\theta + MN d_x}{MN}} h^{1/2}, \quad (37)$$

where the step-size restriction can also be simplified to $0 < h \leq 2/(\mu + L)$. Now, let us denote $\nu_k^\theta = \mathcal{L}(\theta_k)$ and $\pi_\Theta(\theta) = \int \pi(\theta, z^{1:M,1:N}) dz^{1:M,1:N}$, then by the definition of Wasserstein distance

$$W_2(\nu_k^\theta, \pi_\Theta) \leq W_2(\nu_k, \pi).$$

We also note that, due to strong convexity [\(Altschuler and Chewi, 2024, Lemma A.8\)](#)

$$W_2(\delta_{\theta_*}, \pi_\Theta) \leq \sqrt{\frac{d_\theta}{\mu MN}}.$$

Merging these results, we arrive at

$$\mathbb{E} [\|\theta_k - \theta_*\|^2]^{1/2} \leq (1 - \mu h)^k W_2(\nu_0, \pi) + 1.65 \left(\frac{L}{\mu} \right) \sqrt{\frac{d_\theta + MN d_x}{MN}} h^{1/2} + \sqrt{\frac{d_\theta}{\mu MN}}. \quad (38)$$

□

B.2 Preliminary result for Theorem 2

In this section, we rework Theorem 4 in [Dalalyan and Karagulyan \(2019\)](#) in the same assumption setting as in [A3](#). Let $f : \mathbb{R}^p \rightarrow \mathbb{R}$ be a μ -strongly convex function with L -Lipschitz gradients. Let $\vartheta_{k,h}$ denote the iterates of the noisy LMC (nLMC) algorithm as defined in [Dalalyan and Karagulyan \(2019\)](#)

$$\vartheta_{k+1,h} = \vartheta_{k,h} - h \nabla f(\vartheta_{k,h}) + h \zeta_k + \sqrt{2h} \xi_{k+1}; \quad k = 0, 1, 2, \dots \quad (39)$$

where $h > 0$ and ξ_{k+1} are a collection of standard Gaussian random variables of appropriate dimension. Suppose for some $\delta > 0$ and $\sigma > 0$ and for every $k \in \mathbb{N}$, [A3](#) holds for $(\zeta_k)_{k \geq 0}$. We then have the following proposition.

Proposition B.1 (Theorem 4 in [Dalalyan and Karagulyan \(2019\)](#) adapted). *Let $\vartheta_{K,h}$ be the K the iterate of the nLMC algorithm and v_K be its distribution. If the function $f : \mathbb{R}^p \rightarrow \mathbb{R}$ is L -Lipschitz and μ -strongly convex and $h \leq 2/(\mu + L)$ then*

$$W_2(v_K, \pi) \leq (1 - \mu h)^K W_2(v_0, \pi) + 1.65(L/\mu)(hp)^{1/2} + \frac{\delta}{\mu} + \frac{\sigma^2 h^{1/2}}{1.65 L p^{1/2} + \sigma \sqrt{\mu}}$$

Proof. Under [A3](#), modified Proposition 2 in [Dalalyan and Karagulyan \(2019\)](#) yields

$$W_2(\nu_{k+1}, \pi)^2 \leq \left\{ (1 - \mu h) W_2(\nu_k, \pi) + \alpha L (h^3 p)^{1/2} + h \delta \right\}^2 + \sigma^2 h^2 \quad (40)$$

Applying Lemma 1 ([Dalalyan and Karagulyan, 2019](#)) with $A = \mu h$, $B = \sigma h$ and $C = \alpha L (h^3 p)^{1/2} + h \delta$, implies that $W_2(\nu_k, \pi)$ is less than or equal to

$$(1 - mh)^k W_2(\nu_0, \pi) + \frac{\alpha L (hp)^{1/2} + \delta}{\mu} + \frac{\sigma^2 h}{\alpha L (hp)^{1/2} + \delta + (\mu h)^{1/2} \sigma} \quad (41)$$

where $\alpha = 7\sqrt{2}/6 \leq 1.65$. □

B.3 Proof of Theorem 2

Let us define $\tilde{\theta}_k = (\tilde{\alpha}_k, \tilde{\beta}_k)$. We can compactly write (15)–(17) as:

$$\tilde{\theta}_{k+1} = \tilde{\theta}_k - \frac{h}{MN} \sum_{m=1}^M \sum_{n=1}^N \nabla_1 \phi_{y_m}(\tilde{\theta}_k, \tilde{X}_k^{m,n}) + h \zeta_k + \sqrt{\frac{2h}{MN}} W_k, \quad (42)$$

$$\tilde{X}_{k+1}^{m,n} = \tilde{X}_k^{m,n} - h \nabla_2 \phi_{y_m}(\tilde{\theta}_k, \tilde{X}_k^{m,n}) + \sqrt{2h} W_k^{m,n}, \quad (43)$$

where $\mathbb{R}^{d_\theta} \ni \zeta_k = (\zeta_k, 0_{d_\beta})^\top$ and $\zeta_k := \mathbb{E}_{p_{\alpha_k}(x)}[\nabla_\alpha U_{\alpha_k}(x)] - g_k$ for all $k \in \{1, \dots, K\}$ where $g_k := \frac{1}{M} \sum_{m=1}^M \nabla_\alpha U_{\alpha_k}(\tilde{X}_{k,J}^m)$.

Given Proposition B.1, we can follow the same steps as in the proof of Theorem 1 to obtain the bound:

$$\begin{aligned} \mathbb{E} \left[\|\tilde{\theta}_k - \theta_\star\|^2 \right]^{1/2} &\leq (1 - \mu h)^k W_2(\nu_0, \pi) + 1.65 \left(\frac{L}{\mu} \right) \sqrt{\frac{d_\theta + MN d_x}{MN}} h^{1/2} \\ &\quad + \frac{\sigma^2 \sqrt{h}}{1.65 L (MN)^{3/2} \sqrt{d_\theta + MN d_x} + \sigma MN \sqrt{\mu}} + \frac{\delta}{MN \mu} + \sqrt{\frac{d_\theta}{\mu MN}}. \end{aligned} \quad (44)$$

We can then identify

$$\begin{aligned}\tilde{C}_0 &= W_2(\nu_0, \pi), \\ \tilde{C}_1 &= 1.65 \left(\frac{L}{\mu} \right) \sqrt{\frac{d_\theta + MNd_x}{MN}} + \frac{\sigma^2}{1.65L(MN)^{3/2} \sqrt{d_\theta + MNd_x} + \sigma MN \sqrt{\mu}}, \\ \tilde{C}_2 &= \frac{\delta}{\mu} + \sqrt{\frac{d_\theta}{\mu}}.\end{aligned}$$

C Implementation Details

C.1 A Practical Algorithm

We now provide a few modifications to enable efficient simulation of the gradient flow. We include the pseudocode in Algorithm 2.

Subsampling The updates in Eqs. (15)-(17) are prohibitively expensive due to the need of averaging over the entire training set of M data points. Instead, we adopt the mini-batching strategy (Kuntz et al., 2023; Wang et al., 2025) and compute a subsampled version of the losses. For a minibatch of indices $\mathcal{B} \subseteq [M]$, we compute the energy loss and generator loss as:

$$\hat{\mathcal{L}}_d(X^{1:M,1:N}, \mathcal{B}) = \frac{1}{N|\mathcal{B}|} \sum_{(m,n) \in \mathcal{B} \times [N]} V(X^{m,n}, y^m), \quad (45)$$

$$\hat{\mathcal{L}}_e(\hat{X}_J^{1:M}, X^{1:M,1:N}, \mathcal{B}) = \frac{1}{N|\mathcal{B}|} \sum_{(m,n) \in \mathcal{B} \times [N]} U(X^{m,n}) - \frac{1}{|\mathcal{B}|} \sum_{m \in \mathcal{B}} U(\hat{X}_J^m), \quad (46)$$

where $X^{1:M,1:N}$ are the posterior particles, $\hat{X}_J^{1:M}$ are particles sampled from the energy prior using J Langevin steps. This reduces the computational cost for each update to the posterior particles from $\mathcal{O}(MN)$ to $\mathcal{O}(|\mathcal{B}|N)$.

Noise Addition Due to the use of mini-batching, we also adapt the Langevin dynamics to account for the noise added to the posterior particles $X^{1:M,1:N}$. Assume $BL = M$ for some integer L , the generator is updated K times in one epoch, while for each $m \in [M]$, the particle cloud $X^{m,1:N}$ is only updated once. To ensure the particles are not trapped in the local optima after generator updates, we add the Brownian motion scaled by $\sqrt{1/L}$ to all particles every time the generator is updated, which also matches with the amount of noise added in (17). When M is not divisible by the batch size, we take $L = M/B$. Since the noise addition does not involve gradient computations, it is relatively cheap compared to the posterior updates.

Adaptive Optimisers To accelerate convergence, we use the Adam optimiser Kingma and Ba (2014) for the network parameters (α, β) , following the practice in Pang et al. (2020); Schröder et al. (2023). We detail the hyperparameters in Section D.1 and Section D.2.

C.2 EBIPLA with Warmup for Image Experiments

To quickly traverse through the transient phase for the posterior particles in image experiments (Kuntz et al., 2023), we adopt a warm up scheme similar to the predictor-corrector SDE solver in Song et al. (2021), correcting the solution to the posterior SDE in (8) using Langevin dynamics. We apply the warmup during the first 10K training iterations and run the Langevin dynamics for 10 steps. After the warm-up, we initialise $X_{\text{post}}^{m,1:N}$ by creating N identical copies of each $X_{\text{post}}^{m,1}$ obtained from the persistent chains. We provide the pseudocode in Algorithm 3.

Algorithm 2 A practical version of EBIPLA

Require: Number of training iterations K , number of particles N , number of prior iterations J , initial parameters (α_0, β_0) , observed data $\{y^m\}_{m=1}^M$, initial particles $X_0^{1:M,1:N}$, stepsizes $h > 0$ and $\gamma > 0$

- 1: **for** $k = 0$ to $K - 1$ **do**
- 2: Sample batch of indices $\mathcal{B} \subseteq [M]$
- 3: $X_{k+1}^{\mathcal{B},1:N} \leftarrow X_k^{\mathcal{B},1:N} - h \left[\nabla_x U_{\alpha_k}(X_k^{\mathcal{B},1:N}) + \nabla_x V_{\beta_k}(X_k^{\mathcal{B},1:N}, y^{\mathcal{B}}) \right]$ **# Update posterior**
- 4: $X_{k+1}^{1:M,1:N} \leftarrow X_k^{1:M,1:N} + \sqrt{2h/L} \tilde{W}_k^{1:M,1:N}$
- 5: Sample $\hat{X}_{k,0}^{\mathcal{B}} \sim \mathcal{N}(0, I)$
- 6: **for** $j = 0$ to $J - 1$ **do** **# Generate new auxiliary prior samples**
- 7: $\hat{X}_{k,j+1}^{\mathcal{B}} \leftarrow \hat{X}_{k,j}^{\mathcal{B}} - \gamma \nabla_x U_{\alpha_k}(\hat{X}_{k,j}^{\mathcal{B}}) + \sqrt{2\gamma} W_j^{\mathcal{B}}$
- 8: **end for**
- 9: Set $X_{k,J}^{\mathcal{B}} \leftarrow X_{k,J}^{\mathcal{B}}$
- 10: Compute energy loss $\hat{\mathcal{L}}_e = \hat{\mathcal{L}}_e(X_{k,J}^{\mathcal{B}}, X_k^{1:M,1:N}, \mathcal{B})$ in (46)
- 11: Compute generator loss $\hat{\mathcal{L}}_d = \hat{\mathcal{L}}_d(X_k^{1:M,1:N}, \mathcal{B})$ in (45)
- 12: $\alpha_{k+1} \leftarrow \text{OptimizerStep}(\alpha_k, \hat{\mathcal{L}}_e)$
- 13: $\beta_{k+1} \leftarrow \text{OptimizerStep}(\beta_k, \hat{\mathcal{L}}_d)$
- 14: **end for**

C.3 Computational Resources

All experiments were conducted on internal HPCs with NVIDIA L40S (48G) GPUs or servers with NVIDIA RTX 3090 (24G) GPUs.

D Experimental Setup

D.1 Synthetic Experiments

For implementation of EBIPLA on the synthetic dataset we use the practical algorithm as detailed in Section C.1. For fairness of comparison we implement LEBM (Pang et al., 2020) without the prior tilting introduced by the authors. We observed that for our example dataset the tilting which is a form of prior regularisation hindered the performance of both EBIPLA and LEBM and hence decided to drop it for both methods.

Data To create the rotated Swiss roll we sample $t \in [t_{\min}, t_{\max}]$ uniformly in arc length to ensure even distribution of the datapoints. Latent points are $x_{\text{lat}}(t) = \frac{1}{8}[t \cos t, t \sin t] + \varepsilon$, $\varepsilon \sim \mathcal{N}(0, 0.01I)$. We map to the ambient space via a fixed linear decoder $T : \mathbb{R}^2 \rightarrow \mathbb{R}^2$ with orthonormal rows, which results in a rotated Swiss roll (see Figure 5). The dataset size was set to 10000 data points.

Architecture We set the standard deviation of the Gaussian decoder for both models to $\sigma = 0.05$. For the prior energy $U_{\alpha}(x)$ we use a multi-layer perceptron (MLP) with three hidden layers, each with 128 hidden units and SiLU activation for EBIPLA and ReLU activation for LEBM. We observed that ReLU worked better for the baseline method. The generator $g_{\beta}(z) : \mathbb{R}^{d_z} \rightarrow \mathbb{R}^{d_x}$ is a single linear layer mapping.

Training We train both models for 200 epochs with the batch size of 1000 data points. For the parameter updates (α, β) we use the Adam optimiser with learning rate 1×10^{-2} for both. The exponential decay rates for the first and second moment estimates were configured as $\beta_1 = 0.5$ and $\beta_2 = 0.999$, respectively. We vary the prior ULA step size γ and the posterior discretization step

Algorithm 3 A practical version of EBIPLA with warmup

Require: Number of training iterations K , number of prior iterations J , warmup iterations S_{warm} , initial parameters (α_0, β_0) , observed data $\{y^m\}_{m=1}^M$, initial particles $X_0^{1:M, 1:N'}$ with N' , final number of particles N with $N \equiv 0 \pmod{N'}$, stepsizes $h > 0$, $h_{\text{warm}} > 0$, and $\gamma > 0$.

```

1: for  $k = 0$  to  $K - 1$  do
2:   Sample batch of indices  $\mathcal{B} \subseteq [M]$  # Update posterior samples
3:   if  $t < S_{\text{warm}}$  then
4:      $X' \leftarrow X_{\text{warm}, t}^{\mathcal{B}, 1:N'}$ 
5:     for  $i = 1, \dots, 10$  do
6:        $X' \leftarrow X' - h_{\text{warm}} [\nabla_x U_{\alpha_t}(X') + \nabla_x V_{\beta_t}(X', y^{\mathcal{B}})] + \sqrt{2h_{\text{warm}}} \epsilon'$ 
7:     end for
8:      $X_{k+1}^{\mathcal{B}, 1:N'} \leftarrow X'$ 
9:   else if  $k == S_{\text{warm}}$  then
10:    Replicate to  $N$  particles
11:    Set  $N' \leftarrow N$ 
12:   else
13:      $X_{k+1}^{\mathcal{B}, 1:N'} \leftarrow X_k^{\mathcal{B}, 1:N'} - h [\nabla_x U_{\alpha_k}(X_k^{\mathcal{B}, 1:N'}) + \nabla_x V_{\beta_k}(X_k^{\mathcal{B}, 1:N'}, y^{\mathcal{B}})]$ 
14:      $X_{k+1}^{1:M, 1:N'} \leftarrow X_k^{1:M, 1:N'} + \sqrt{2h/L} \tilde{W}_k^{1:M, 1:N'}$ 
15:   end if
16:   Sample  $\hat{X}_{k,0}^{\mathcal{B}} \sim \mathcal{N}(0, I)$ 
17:   for  $j = 0$  to  $J - 1$  do # Generate new auxiliary prior samples
18:      $\hat{X}_{k,j+1}^{\mathcal{B}} \leftarrow \hat{X}_{k,j}^{\mathcal{B}} - \gamma \nabla_x U_{\alpha_k}(\hat{X}_{k,j}^{\mathcal{B}}) + \sqrt{2\gamma} W_j^{\mathcal{B}}$ 
19:   end for
20:   Set  $X_{k,J}^{\mathcal{B}} \leftarrow \hat{X}_{k,J}^{\mathcal{B}}$ 
21:   Compute energy loss  $\hat{\mathcal{L}}_e = \hat{\mathcal{L}}_e(X_{k,J}^{\mathcal{B}}, X_k^{1:M, 1:N'}, \mathcal{B})$  in (46)
22:   Compute generator loss  $\hat{\mathcal{L}}_d = \hat{\mathcal{L}}_d(X_k^{1:M, 1:N'}, \mathcal{B})$  in (45)
23:    $\alpha_{k+1} \leftarrow \text{OptimizerStep}(\alpha_k, \hat{\mathcal{L}}_e)$ 
24:    $\beta_{k+1} \leftarrow \text{OptimizerStep}(\beta_k, \hat{\mathcal{L}}_d)$ 
25: end for

```

size h in EBIPLA, as well as the prior γ and posterior h ULA step sizes in LEBM, according to the number of posterior particles or MCMC steps (see Table 2).

Evaluation We report the MMD (Gretton et al., 2012) between the generated samples and the ground truth on the rotated Swiss roll. For samples $\{x_i\}_{i=1}^m \sim P$ and $\{y_i\}_{j=1}^n \sim Q$, the unbiased Monte-Carlo estimate of MMD is defined as:

$$\text{MMD}(P, Q) \approx \frac{1}{m(m-1)} \sum_{i=1}^m \sum_{\substack{j=1 \\ j \neq i}}^m k(x_i, x_j) + \frac{1}{n(n-1)} \sum_{i=1}^n \sum_{\substack{j=1 \\ j \neq i}}^n k(y_i, y_j) - \frac{2}{mn} \sum_{i=1}^m \sum_{j=1}^n k(x_i, y_j), \quad (47)$$

where we use the Radial Basis Function (RBF) kernel $k : \mathbb{R}^{d_x} \times \mathbb{R}^{d_x} \rightarrow \mathbb{R}_{\geq 0}$ with a bandwidth $\gamma = 0.1$ defined as $k(x, y) = \exp(-\gamma \|x - y\|^2)$. A total of 1000 samples were generated via 500 prior Langevin dynamics and then passed through generator. We repeat the training runs with 20 different random seeds and report in Figure 2 the mean and standard error.

D.2 Image Experiments

Model and Architecture. We set the standard deviation of the Gaussian decoder to $\sigma = 0.3$ following Pang et al. (2020). The architecture of the energy and generator networks are also chosen

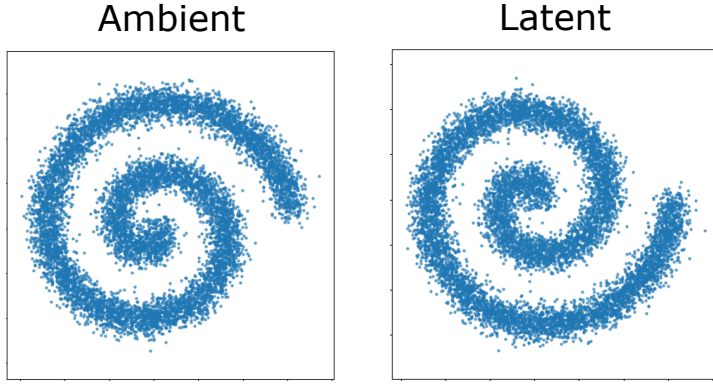


Figure 5: Visualisation of the rotated Swiss roll dataset

Table 2: Step sizes used for the prior and posterior updates in EBIPLA and LEBM. For LEBM, N denotes the number of posterior particles (EBIPLA) or MCMC steps (LEBM)

| N | EBIPLA | | LEBM | |
|-----|----------|-----|----------|-------|
| | γ | h | γ | h |
| 4 | 0.005 | 0.9 | 0.003 | 0.005 |
| 16 | 0.007 | 0.9 | 0.006 | 0.005 |
| 32 | 0.007 | 0.9 | 0.002 | 0.005 |
| 64 | 0.009 | 0.9 | 0.005 | 0.02 |

to be the same as [Pang et al. \(2020\)](#) to ensure a fair comparison.

Training. We train EBIPLA on all datasets for 200 epochs with a batch size of 128. We use the Adam optimiser for both the energy and generator networks: for the energy network, we use a learning rate of 2×10^{-4} and set $(\beta_1, \beta_2) = (0.5, 0.999)$, for the generator we use a learning rate of 1×10^{-3} and $(\beta_1, \beta_2) = (0.9, 0.999)$; an exponential learning rate schedule with rate 0.999 was used for both networks. The warmup is applied during the first $10K$ iterations of the training with $h_{\text{warm}} = 0.005$ (cf. Section C.2). For particle updates, we choose $\gamma = 0.1$ and $h = 0.1$.

Evaluation. For the computation of FID values, we sample 50,000 from the energy based prior using 60 steps; we select the step size for different datasets using grid search over values $\{0.01, 0.05, 0.07, 0.1, 0.2\}$. We use a step size of 0.07 for SVHN and step size 0.1 for CelebA64 and CIFAR10.

For the evaluation of reconstruction error, we use the similar set up in [Kuntz et al. \(2023\)](#) and compute the maximum a posterior (MAP) estimate for the latents x^m corresponding to each y^m in the validation set:

$$x_{\text{map}}^m = \arg \max_{x \in \mathbb{R}^{d_x}} \log p(x|y^m) = \arg \min_{x \in \mathbb{R}^{d_x}} \frac{1}{2\sigma^2} \|y^m - g_\beta(x)\|_2^2 + U_\alpha(x).$$

Then, we recover the image by mapping x_{map}^m through the generator. To solve MAP estimation problem above, we use 4 randomly initialised runs of Adam ([Kingma and Ba, 2014](#)) of length 50 iterations and set the learning rate using PyTorch’s `ReduceLROnPlateau` scheduler with an initial learning rate of 1; all other Adam parameters are set to the defaults.